Elastic interaction between CuCl nanocrystals and a matrix of crystalline NaCl

H.-J. Weber,[1] J. Schreuer,[2] and C. Popa-Varga[1]
[1]*Institut für Physik, Universität Dortmund, D-44221 Dortmund, Germany*
[2]*Laboratory of Crystallography, ETH Zürich, Switzerland*
(Received 26 January 2004; revised manuscript received 15 April 2004; published 30 June 2004)

CuCl nanocrystals embedded in single crystals of NaCl are used as a model system to study interfacial elastic forces and to compare experimental results with the predictions of elastic continuum theory. The concentration of nanocrystals and the stress they are feeling are measured by exciton spectroscopy. Elastic constants are determined with remarkable accuracy by resonant ultrasound spectroscopy. All measurements show significant changes of optical and elastic properties above $T_c \approx 333$ K. They are a consequence of a sudden increase of cation mobility. Depending on the original state of a sample, the result is a spontaneous nucleation of nanocrystals or a weakening of interfacial forces above T_c. Two elastic phenomena are observed that do not exist in pure NaCl. The first one shows the signature of an elastic fluid: $c_{fl}=c_{11}=c_{12}$ and $c_{44}=0$. The second one appears as the increment Δc^* of the difference $c_{11}-c_{12}$ above T_c. The changes of optical and elastic properties observed in two samples being in different thermodynamic states are consistently described by a modified elastic continuum theory.

DOI: 10.1103/PhysRevB.69.235419 PACS number(s): 61.46.+w, 78.67.Bf, 62.25.+g

I. INTRODUCTION

Electronic properties of semiconductor nanocrystals or quantum dots are modified by the quantum-confinement effect.[1,2] The resulting new linear and nonlinear optical properties are a subject of current interest and a lot of new phenomena have been observed for CuCl nanocrystals embedded in NaCl (abbreviated as CuCl:NaCl in the following).[3] Interpretations of optical experiments that probe electronic properties of quantum dots usually ignore their coupling to the surrounding. But this coupling is important. It is needed to handle nanocrystals in experimental work and sometimes it is used to explain the occurrence of self-assembled quantum dots.[4] The standard treatment of interactions between nanocrystals and their surrounding is based on the continuum theory of elasticity.[4,5] An impressive example of the importance of built-in stresses and strains is the dense quantum dot arrays, which are believed to exist only due to the stabilization by strains.[6] Elastic interactions in heterogeneous material are mainly considered theoretically because their experimental detection is difficult. Therefore, it seems to be an open question whether the widely used continuum theory of elasticity describes the reality on the nanometer scale of heterogeneous materials completely. The main aim of the present work is to clarify this question.

In contrast to epitaxially grown semiconductor systems, CuCl nanocrystals nucleate in a NaCl single crystal as a consequence of a thermodynamically driven phase separation. Therefore, the built-in strain is not needed to explain their stability. Another advantage of the system is the chemical variability. CuCl may be replaced by CuBr, CuI, and the corresponding silver halides,[7] and the matrix can consist of different alkali halides. The chemical variability permits the systematic study of interactions between nanocrystals and crystalline matrices and the tailoring of materials with respect to properties resulting from this interaction. However, the main advantage of CuCl:NaCl for our purpose is the possibility to prepare large samples. They are needed to measure average elastic and optical properties with high accuracy.

In CuCl:NaCl, the concentration of crystalline CuCl molecules is less than 10^{-3}.[8] As a consequence of low doping, it is possible to observe elastic mechanisms which are related to well-separated basic units. They will be called elastic domains. The small concentration and the small sizes of nanocrystals make the detection of effects difficult, which can be traced back to the impact of embedded crystals. An experimental technique of high sensitivity and accuracy is resonant ultrasound spectroscopy (RUS).[9,10] Evidence for elastic interaction between CuCl nanocrystals and the NaCl matrix was observed previously by RUS measurements on samples of different thermal history.[11] The previous experiments also revealed the crucial influence of sample imperfections which may even prevent the evaluation of reliable results. To increase experimental reliability, we now perform elastic measurements as a function of temperature. In this way, the influence of the sample irregularities which do not depend on temperature is removed. Furthermore, elastic measurements are complemented by optical ones. As is well known, exciton spectroscopy in CuCl:NaCl can be used to study thermodynamic and kinetic phenomena in the course of phase-separation processes.[8] Here we also use the effect that spectral positions of excitons depend not only on the size of the nanocrystals but also on the stress they are feeling. A further improvement of experimental reliability has been achieved by using two types of samples which are in different states due to a different thermal history. Samples of the first type are saturated with nanocrystals at the growth temperature $T_{gr}=376$ K and become unstable at high temperatures. Samples of the second type are made from quenched as-grown single crystals. They contain no or only a few nanocrystals and become stable upon warming up because the strong increase of ionic mobility stimulates the nucleation and the growth of nanocrystals.

Section II presents a model of elastic interaction between a nanocrystal and the surrounding matrix which is based on the elastic continuum theory. Such a theory is of particular simplicity in CuCl:NaCl because the small concentration of nanocrystals guarantees that coupling between them is of no importance. Experimental details are given in Sec. III and the results of elastic and optical measurements are presented in Sec. IV. In Sec. V, experiments are analyzed and discussed, and in Sec. VI those results are emphasized that are believed to be of general importance.

II. MODEL OF ELASTIC INTERACTION

A. Basic equations

The lattice constant of bulk CuCl ($a_0^*=0.5416$ nm) is smaller than that of pure NaCl ($a_0=0.564$ nm). Therefore, without any relaxation a spatial gap would appear between CuCl nanocrystals and the surrounding matrix if they are embedded in a single crystal of NaCl. However, strong forces between nanocrystals and the matrix reduce or even close the gap. The existence of such forces is expected because both chemical components possess the same fcc sublattice of their anions. This view is supported by the results of two-photon absorption experiments, which show that the crystallographic orientations of guest and host coincide.[12] Our description of elastic interactions begins with a hypothetical situation. A spherical nanocrystal already exists. Its lattice parameter is a_0^* and it is surrounded by the interfacial gap and by the matrix of NaCl which contains the residual copper ions. We assume that both materials behave like elastic isotropic ones as long as only spontaneous forces and effects are treated, which is the case in the present section. Now we consider the local stresses T_{ij} and strains S_{ij} in the vicinity of a nanocrystal. They are described in terms of spherical coordinates with the origin in the center of the nanocrystal. Using Hook's law and expressing strains in terms of displacement $\vec{u}$, elastic equilibrium is written as[13]

$$\vec{\nabla}\cdot(\vec{\nabla}\cdot\vec{u})=0. \tag{1}$$

Due to the spherical symmetry, radial displacements u_r are the only type of displacements that can occur. In this case, Eq. (1) is solved by

$$u_r=ar+\frac{b}{r^2}. \tag{2}$$

Elastic strains are related to these displacement by

$$S_r=\frac{\partial u_r}{\partial r}=a-2\frac{b}{r^3},\quad S_\Theta=S_\Phi=\frac{u_r}{r}=a+\frac{b}{r^3}. \tag{3}$$

Here and in the following, the condensed matrix notation is applied. Superscripts "NC" and "M" will be used to characterize quantities that belong to nanocrystal and matrix, respectively. The parameters a and b in Eq. (3) are determined by boundary conditions. One condition is $u_r^{\mathrm{NC}}=0$ at $r=0$. This is consistent with $b^{\mathrm{NC}}=0$, which in turn is equivalent to a homogeneous deformation of nanocrystals. Parameters a^M and b^M of the matrix are both nonzero. Of special importance are the invariants $S_0=(S_r+S_\Theta+S_\Phi)/3$ and $T_0=(T_r+T_\Theta+T_\Phi)/3$. They describe two basic quantities, namely relative changes of volume and negative hydrostatic pressure. Notice that $S_0=a$ is valid even in the matrix in which the $1/r^3$ terms do not vanish [see Eq. (3)]. Hook's law for these components reads

$$T_0=C_{01}S_0, \tag{4}$$

where $C_{01}=c_{rr}+2c_{r\Theta}=c_{11}+2c_{12}$ is one of the two scalar invariants of the elastic tensor. In the present section, we use the relations $c_{rr}=c_{\Theta\Theta}=c_{\Phi\Phi}=c_{11}$ and $c_{r\Theta}=c_{r\Phi}=c_{\Theta\Phi}=c_{12}$. They are indicative of elastic isotropy.

In conclusion, the elasticity of a nanocrystal is described by

$$T_0^{\mathrm{NC}}=T_r^{\mathrm{NC}}=T_\Theta^{\mathrm{NC}}=T_\Phi^{\mathrm{NC}}=C_{01}^{\mathrm{NC}}a^{\mathrm{NC}}. \tag{5}$$

The corresponding equations for the surrounding matrix read

$$T_r^M=\left[C_{01}a-2(c_{11}-c_{12})\frac{b}{r^3}\right]^M,$$

$$T_\Theta^M=T_\Phi^M=\left[C_{01}a+(c_{11}-c_{12})\frac{b}{r^3}\right]^M,$$

$$T_0^M=C_{01}^Ma^M. \tag{6}$$

B. Elastic domains

The idealized structural unit of the composite material is a sphere of radius R_b. Its center is occupied by a spherical nanocrystal which is surrounded by the matrix consisting of NaCl doped by the residual copper ions of the molar fraction x_i. The radius of the nanocrystal is R_0 and the magnitude of R_b is approximately $R_b\approx R_0/(x_{\mathrm{cr}})^{1/3}$, where x_{cr} denotes the molar fraction of CuCl in the crystalline state.

Assuming the validity of Vegard's rule, the lattice constant of the matrix, which is a solid solution, is written as

$$a_{\mathrm{ss}}=a_0\left[1-x_i\left(\frac{a_0-a_{\mathrm{hyp}}}{a_0}\right)\right], \tag{7}$$

where a_{hyp} corresponds to a hypothetical CuCl crystal of rock salt structure. Without any elastic interaction between nanocrystal and matrix, the misfit $a_{\mathrm{ss}}-a_0^*\approx a_0-a_0^*$ would produce the spatial gap ΔR. This interaction is described by the interfacial stresses

$$T_{r,0}^{\mathrm{NC}}=T_{r,0}^M(r=R_0), \tag{8}$$

where $T_{r,0}^{\mathrm{NC}}$ and $T_{r,0}^M$ are given by Eqs. (5) and (6). A consequence of these stresses is displacements $u_{r,0}^M$ and $u_{r,0}^{\mathrm{NC}}$ at the interface. They close the gap, which leads to the second boundary condition,

$$a^{\mathrm{NC}}-a^M-\frac{b^M}{R_0^3}=\frac{\Delta R}{R_0}. \tag{9}$$

Here $\Delta R/R_0=0.041$ is the maximal possible value due to the lattice misfit. As the signs of the parameters a^M and b^M

should be the same, the radial stress must change its sign at a distance R_α between R_0 and R_b,

$$T_{r,\alpha} = 0 (r = R_\alpha \quad \text{with } R_0 < R_\alpha < R_b). \tag{10}$$

Equations (8)–(10) are used to express the material parameters a^{NC}, a^M, and b^M/R_0^3 in terms of $\Delta R/R_0$, R_b/R_α, x_{cr}, and elastic constants. In case of a pure elastic medium, the deformation energy should show a minimum which results in $R_\alpha = R_b$ for the present model.

C. Numerical estimates and features of experimental methods

Nucleation and growth of nanocrystals are accompanied by two different processes: (α) The volume of the matrix increases because the concentration of ionic copper decreases [see Eq. (7)].

(β) There is a closing of the gaps that are produced by the lattice misfits between CuCl nanocrystals and the NaCl matrix.

Assuming that the lattice parameter of LiCl, hypothetical CuCl, and NaCl vary linearly with the radii of cations, we obtain by use of modified Shannon radii[14] $(a_0 - a_{\mathrm{hyp}})/a_0 = 0.079$. This value is assumed to represent the upper limit of the contraction of pure NaCl by doping with copper ions. Now a numerical estimate of strains is carried out by use of data which correspond to sample SE1 (see Sec. III). The strain according to process (α) is $S_0^\alpha = 2.4 \times 10^{-5}$. The maximal strain according to process (β) occurs if the whole free volume of gaps is transferred into a compression of the matrix: $S_0^\beta = -0.002$. This value is not consistent with the elastic model outlined above. The real strain will be smaller, but it will be negative. Thus, two compensating effects will superpose. These considerations show that the detection of S_0 needs an extraordinarily high experimental sensitivity.

A highly sensitive probe for the investigation of elastic properties is provided by resonant ultrasound spectroscopy (RUS), where the elastic constants of a crystal are derived from an experimentally measured ultrasonic resonance spectrum of a freely vibrating sample with a well-defined shape. The main advantages offered by RUS are (i) all independent elastic constants can be studied simultaneously on one sample, (ii) no medium is required for transducer sample coupling, and (iii) the resulting sample parameters show a high internal consistency.[15] The accuracy of the RUS technique is mainly limited by errors of the sample dimensions, deviations from the ideal geometry, and violations of the free boundary conditions due to sample mounting. The influence of these error sources on the observed resonance frequencies should be independent of temperature. Therefore, sensitivity can even be improved by considering variations of the resonance frequencies of a sample as a function of temperature.

Whereas the average strain S_0 is so small that its experimental detection is hard to realize, the radial stress at the nanocrystal-matrix interface is rather big. We calculate for the reference sample SE1 the tensile stress $T_{r,0} = 1.8$ GPa. Because it is strongly localized to the near neighborhood of nanocrystals and because it is accompanied by a corresponding transversal pressure, no direct impact of $T_{r,0}$ on the observable elastic constants is expected.

To observe the local stress, a local probe is needed. This can be exciton spectroscopy. In bulk CuCl, hydrostatic pressure of 1 GPa produces a blueshift of both excitons of 7.65 meV.[16] In CuCl:NaCl, 7.9 meV/GPa (12.0 meV/GPa) was observed on samples containing nanocrystals of $R_0 = 10$ nm($R_0 = 1.5$ nm).[17] Thus, exciton spectroscopy and RUS provide us with complementary information concerning the existence of built-in stresses.

III. EXPERIMENT

A large single crystal of CuCl-doped NaCl was grown by the Czochralski technique. Two rectangular parallelepipeds with {100}-faces suitable for elastic measurements and two thin plates were prepared from the bowl. One parallelepiped (sample SE1) and one plate (sample SO1) were heated to 650 K. At this temperature, all copper is in the state of randomly distributed ions at cation sites of NaCl. Then both samples were annealed for 48 h at 376 K to nucleate and grow nanocrystals.[18] Neither the second parallelepiped (sample SE2) nor the second plate (sample SO3) were subjected to any thermal treatment. SE2 was used for elastic measurements at room temperature only. After these measurements it was divided into two parts. One part (sample SE3) was used for elastic measurements as a function of temperature. Optical-absorption measurements were performed on the two plates SO1 and SO3.

The RUS apparatus was designed to achieve a thermal stability of at least ±0.1 K in the temperature range between 250 K and 400 K. The samples prepared as rectangular parallelepipeds were weakly clamped at two opposite corners by alumina buffer rods which act simultaneously as sample holder and as ultrasonic waveguides. Two piezoelectric transducers operating as ultrasound generator and detector, respectively, were glued to the end of the buffer rods outside the cooled/heated area. Between 130 and 400 kHz, about 40 eigenresonances of each sample have been observed. The resonance frequencies serve as raw data for the determination of elastic constants by assuming cubic symmetry. To check the experimental limits, we measured the elastic constants at room temperature of sample SE2 and of sample SE3 before and after it was cooled down to 278 K. The results are $c_{11} = 49.53(5)$ GPa, $c_{12} = 12.93(4)$ GPa, and $c_{44} = 12.79(1)$ GPa. The uncertainty of our results is much smaller than the scatter of literature values for pure NaCl obtained by different experimental techniques.[19] The average values reported in literature are $c_{11} = 49.1(5)$GPa, and $c_{12} = c_{44} = 12.8(1)$GPa. Here and in the following, noted errors of n measurements are calculated according to $\sigma = [(1/n)\Sigma(x - \overline{x})^2]^{1/2}$. As the parameter c_{44} is of minor importance, in the present investigation we consider an uncertainty of about ±0.05 GPa as the experimental limit.

Recently, Yamamoto *et al.*[20] presented RUS measurements on pure NaCl between room temperature and 770 K. Below 420 K, the thermal parameters dc_{ij}/dT are constant within experimental error. Therefore, in the present investigation deviations from the linear dependence of resonance frequencies or elastic constants on temperature are the most significant effects which have to be detected. An illustrative

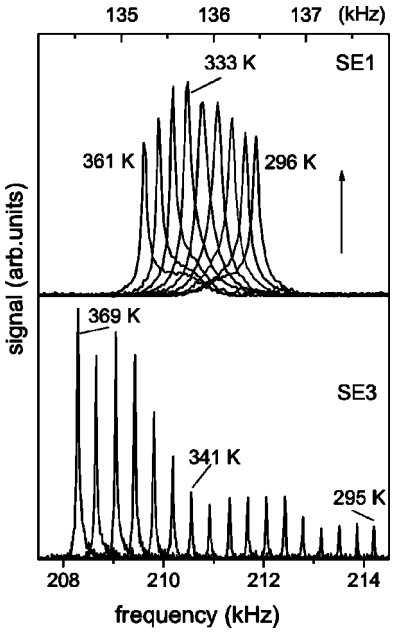

FIG. 1. Examples of ultrasound resonances for different temperatures in samples SE1 and SE3. Average distances between two successive resonances are 8.1 K for SE1 and 4.6 K for SE3.

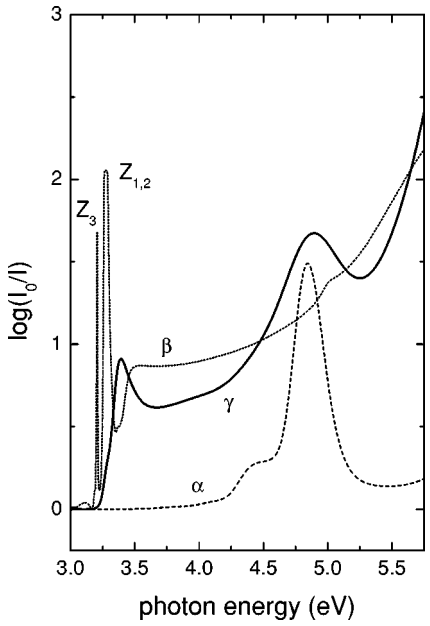

FIG. 2. Absorption spectra of (α) NaCl crystal containing Cu^+ ions at 20 K, (β) crystalline CuCl film on a NaCl substrate at 20 K, and (γ) CuCl:NaCl sample at 294 K. Z_3 and $Z_{1,2}$ denote the two excitons of crystalline CuCl. In the spectrum γ both structures are strongly broadened.

example is presented in Fig. 1. The positions of one resonance peak taken from the spectra of sample SE1 as well as of SE3 are shown for different temperatures. There are two reasons for the shifts of peak positions towards smaller frequencies with increasing temperatures. The first reason is the increase of volume due to thermal expansion. The second reason is the dependence of elastic constants c_{ij} on temperature. Figure 1 also shows rather sudden changes of the amplitudes in both crystals nearly at the same temperature of about 333 K. These changes are indicative of the existence of a thermal anomaly.

The characteristic features of optical spectra are illustrated in Fig. 2. Spectra α, β, and γ represent the dependence of absorption on the photon energy $E=\hbar\,\omega$ of Cu^+ ions in NaCl at 20 K, of a crystalline CuCl film at 20 K, and of CuCl:NaCl at room temperature. Signatures of Cu^+ ions are two broadbands at 4.40 eV and 4.85 eV.[21] The most significant features of crystalline CuCl are the two excitons Z_3 and $Z_{1,2}$ near 3.3 eV.[22] The exact spectral positions E_3 and $E_{1,2}$ of excitons are mainly a function of temperature T and of the size of nanocrystals.[23,24] With increasing T and with decreasing radius R_0 of nanocrystals, E_3 and $E_{1,2}$ shift to larger photon energies. The width of exciton lines depends on temperature and on the size distribution of nanocrystals. Determining the ionic and crystalline contribution to absorption above 3.7 eV separately, the concentrations x_i and x_{cr} of both components of CuCl have been obtained. In the studied sample SO1, which corresponds to the sample SE1 used in elastic measurements, the mole fractions are $x_i=4.4\times10^{-4}$ and $x_{cr}=3.1\times10^{-4}$.

IV. EXPERIMENTAL RESULTS

A. Elasticity

Figure 1 gives some evidence for a thermal anomaly at $T_c\approx333$ K, but the hard experimental data in RUS measurements are not the amplitudes but the resonance frequencies f_i. We have fitted the experimental data f_i below T_c to a linear temperature dependence to obtain theoretical values f_i^f for the whole temperature range under consideration. Figure 3 shows the relative differences $\Delta f_i=(f_i-f_i^f)/f_i$ as a function of temperature. The existence of a characteristic temperature, T_c is obvious. The decrease of resonance frequencies above

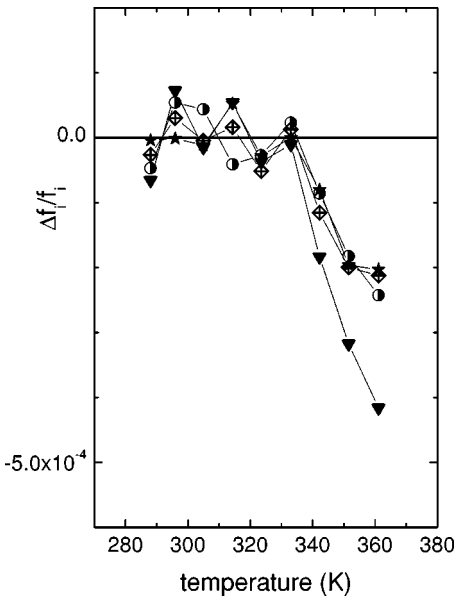

FIG. 3. Relative differences of four resonances as defined in the text as a function of temperature observed in sample SE1. The resonance frequencies are approximately 163 kHz (circles), 244 kHz (triangles), 330 kHz (diamonds), and 372 kHz (stars).

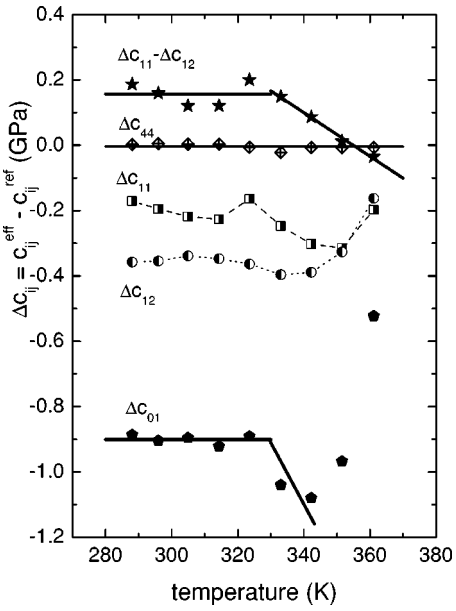

FIG. 4. Differences $\Delta c_{ij}=c_{ij}^{\mathrm{eff}}-c_{ij}^{\mathrm{ref}}$ of elastic constants of sample SE1 as a function of temperature. c_{ij}^{eff} are experimental data and c_{ij}^{ref} are the data of pure NaCl (Ref. 20). Squares: Δc_{11}, circles: Δc_{12}, diamonds: Δc_{44}, stars: $\Delta c_{11}-\Delta c_{12}$, and hexagons: ΔC_{01}. Horizontal full lines represent least squares fits of data obtained below T_c =330 K. The line above T_c is a least-squares fit in the case of $\Delta c_{11}-\Delta c_{12}$ and a guide to the eye in the case of C_{01}. Broken and dotted lines are guides to the eye.

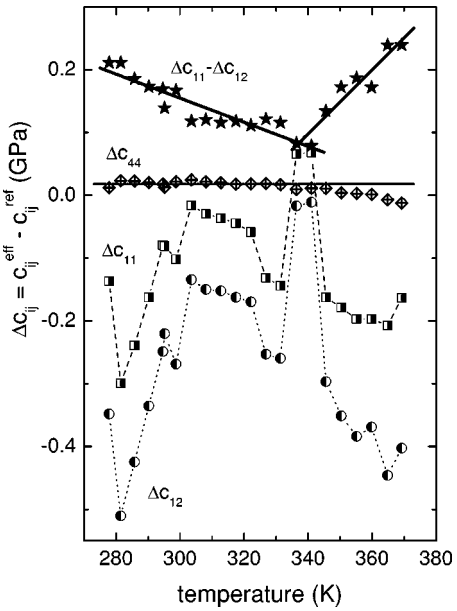

FIG. 5. Differences $\Delta c_{ij}=\Delta c_{ij}^{\mathrm{eff}}-c_{ij}^{\mathrm{ref}}$ of elastic constants of sample SE3 as a function of temperature. Only values of $\Delta c_{11}-\Delta c_{12}$ show a linear dependence on temperature whereby the slopes are different below and above T_c=337 K. For further explanations, see the caption of Fig. 4.

T_c indicates an elastic softening. Figure 3 also demonstrates that the relative accuracy is as high as 5×10^{-5}, which is the average deviation of the data below T_c from the linear T dependence.

Because of the high accuracy of the experimental results, it is not astonishing that the scattering of data reported by different authors is larger than the deviation of our own data from the averaged ones listed by *Landolt-Börnstein*.[19] We use the elastic coefficients of NaCl reported by Yamamoto *et al.*[20] as reference values because these authors worked with the same technique as we did. Subtracting the reference values from our experimental ones, several new features are revealed. $\Delta c_{ij}=c_{ij}$(experimental)$-c_{ij}$(reference) of sample SE1 and SE3 are presented in Figs. 4 and 5. Δc_{44} is approximately equal to zero for the whole temperature range in both samples. Δc_{11} and Δc_{12} are influenced by an additional effect that appears as a kind of statistical scattering, in particular in Fig. 5. This additional effect is absent in the differences $\Delta c_{11}-\Delta c_{12}$, which are included in Figs. 4 and 5. In both cases, these differences show a characteristic temperature, which is T_c=330 K for sample SE1 and T_c=337 K for sample SE3. Above and below T_c, the dependence of $\Delta c_{11}-\Delta c_{12}$ on temperature is linear. In both samples, deviations from linearity are smaller than 0.05 GPa, which has been assumed to be the limit of reliability of the results (see Sec. III). In the following, the changes of $\Delta c_{11}-\Delta c_{12}$ above T_c will be addressed as Δc^{*}. It is given by

$$\frac{\partial \Delta c^{*}}{\partial T}=\frac{\partial (\Delta c_{11}-\Delta c_{12})}{\partial T}=-6.7[7.1]\ \mathrm{MPa/K}. \qquad (11)$$

Here the first number corresponds to sample SE1 and the number in brackets to sample SE3.

The strictly linear dependence of $\Delta c_{11}-\Delta c_{12}$ on temperature demonstrates that the additional effect, which is characterized by anomalous fluctuations with temperature, is equal in Δc_{11} and Δc_{12}. In addition, it is absent in Δc_{44}. This symmetry behavior is just the signature of an *elastic fluid*. Its contribution to the total elastic constant is called here c_{fl}.

Figure 4 also shows ΔC_{01}. For $T>T_c$, there are obviously two contributions, a negative and a positive one. The latter increases in a strongly nonlinear way with temperature. This contribution is therefore assumed to be the elastic-fluid effect. The negative contribution is attributed to the same mechanism which is responsible for the second additional elastic effect Δc^{*}.

B. Exciton absorption

Figure 2 demonstrates strong differences of the exciton spectrum at low and ambient temperature. Reasons are the spectral shifts of excitons towards the short-wavelength range and the increase of linewidths with increasing temperature. Both thermal effects are a consequence of electron-phonon interaction. Figure 6 illustrates exciton absorption of sample SE1 above room temperature. Between 295 K and 401 K, all absorption curves coincide at the nodal point ϵ_0 =3.248(3)eV. Valov *et al.*[25] observed such a nodal point in CuCl nanocrystals embedded in a glass matrix. They argued

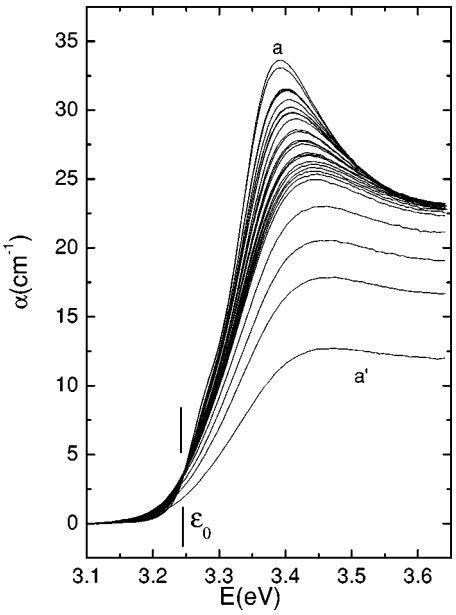

FIG. 6. Absorption coefficient α versus photon energy E of CuCl:NaCl (sample SO1) for different temperatures. The lowest temperature is 295.7 K (curve a) and the highest temperature is 422 K (curve a'). ϵ_0 indicates a nodal point discussed in the text.

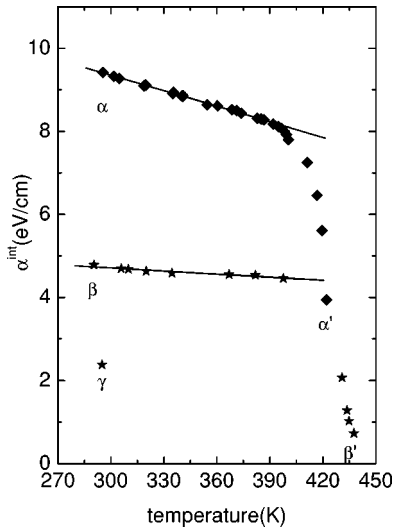

FIG. 7. Integrated absorption of CuCl:NaCl (sample SO1) as defined by Eq. (12) for two subsequent temperature cycles $\alpha \rightarrow \alpha'$ and $\beta \rightarrow \beta'$. Data points α and α' correspond to curves a and a' in Fig. 6.

that ϵ_0 represents the convergent point of the Urbach tail.[26] We have checked that our data obey the Urbach rule for $E \leqslant \epsilon_0$, which supports the interpretation of Valov *et al.*[25] However, the main part of exciton absorption occurs for $E > \epsilon_0$. Therefore, we describe the low-energy side of $\alpha(E)$ in a different way than on the basis of an Urbach tail analysis.

As a measure of the concentration of CuCl crystals, we use the integrated absorption

$$\alpha^{\text{int}} = \int_{3.1}^{3.64} \alpha(E) dE. \tag{12}$$

The high-energy limit of 3.64 eV has been selected as a suitable boundary between exciton and continuous interband absorption. Figure 7 presents α^{int} of the sample SO1 for two temperature cycles. In the first cycle, heating has been finished at 422 K (point α') and then the sample was cooled down to ambient temperature. After this first cycle, the concentration of nanocrystals was smaller than at the beginning because a part of the nanocrystals were dissolved now. A second cycle was stopped at 438 K (point β'). Finally, 25% of the original nanocrystals was left (point γ). The first cycle should reflect the anomaly at the critical temperature T_c if the changes observed in the elastic measurements are caused by the dissolution of the nanocrystals. Instead of this behavior, α^{int} decreases with a constant slope up to about 393 K. The linear decrease with temperature is mainly caused by thermal shifting. Obviously dissolution happens above 393 K.

Room temperature is already sufficiently low to observe the position of the Z_3 exciton by use of the second derivatives of the original curves. We obtained $E_3 = 3.279$ eV, 3.277 eV, and 3.265 eV for the three points α, β, and γ in Fig. 7. In bulk crystals, the corresponding value is $E_3^b = 3.259$ eV. The blueshifts in CuCl:NaCl are used to calculate the average radii of nanocrystals.[8,23,24] Results are $R_{0,\alpha} = 2.7$ nm, $R_{0,\beta} = 2.8$ nm, and $R_{0,\gamma} = 3.7$ nm. The latter value has been checked at 20 K, where exciton peaks are more narrow and therefore better resolved than at room temperature. Results obtained at both temperatures agree within 0.2 nm. The increase of radius R_0 is a consequence of the Gibbs-Thomson effect, which predicts for a small particle size a reduced melting temperature.[27] Thus, at first mainly the small nanocrystals are dissolved and the bigger ones are left. Notice the rather small difference between $R_{0,\alpha}$ and $R_{0,\beta}$ and the smaller decrease of absorption in the second run. Both effects are due to the phenomenon that in the first run mainly the very small nanocrystals have been dissolved. In conclusion, Fig. 7 does not indicate any anomaly at T_c.

Finally, we consider absorption of the long-wavelength side. $\alpha(E)$ in the range $E < (E_{\max} + \delta E)$, is used to fit the area, the central photon energy $E_{\max}$, and the bandwidth of a Gauss function. δE is of the order of a few meV. These fits describe $\alpha(E)$ very well for $E < E_{\max}$, as illustrated in the inset of Fig. 8. The areas turn out to be constant up to 398 K, which agrees with the constant slope of $\alpha^{\text{int}}(T)$ in Fig. 7. The dependence of $E_{\max}$ on temperature is presented in Fig. 8. The slope increases at $T_c \approx 338$ K, which is very near to the onset of anomalies in elastic measurements. Only a change of the interfacial stress $T_{r,0}$ between nanocrystals and matrix is able to describe all phenomena observed at T_c. Figure 8 demonstrates a change of the slope of $\Delta(\partial E/\partial T) = 0.077(7)\text{meV/K}$. This corresponds to

$$\frac{\partial T_{r,0}}{\partial T} = -8.4 \text{ MPa/K}. \tag{13}$$

The negative sign indicates a decrease of the tensile stress which is acting on the nanocrystals already below T_c.

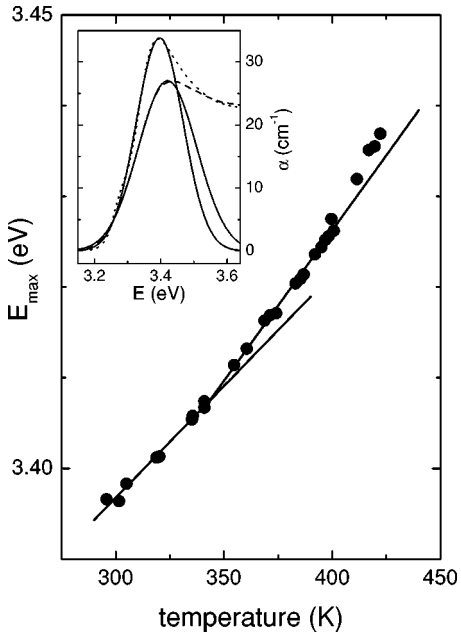

FIG. 8. Spectral position of the $Z_{1,2}$ exciton of sample SO1 as a function of temperature demonstrating changes of the slope. Solid lines are fits to a limited temperature range. The inset illustrates fitted Gauss curves to the low-energy side of spectra for 295.7 K (dotted line) and 383 K (broken line). The latter fit also shows the reduced accuracy of fits at high temperatures. Therefore, the change of slope at about 410 K is not necessarily real.

The optical phenomenon which could be detected with sample SO3 reliably is an increases of α^{int} above T_c. From these data, the concentration of crystalline CuCl at 373 K was determined to be 5×10^{-5}. The value of T_c, was within experimental accuracy, the same as in the elastic measurements.

V. ANALYSIS OF RESULTS AND DISCUSSION

A. Elastic-fluid phenomenon

Our experiments demonstrate the existence of two additional elastic effects which are absent in pure NaCl and which are both related to the characteristic temperature T_c. Most curious is the appearance of a phenomenon that shows the symmetry of a fluid. In particular, Fig. 5 (sample SE3) indicates irregularities of the dependence of c_{fl} on temperature. This finding is consistent with the following observation we made several times in CuCl:NaCl. A sample which is prepared from an as-grown crystal does not show narrow exciton lines at low temperature, which indicates the absence of well-grown nanocrystals. Most probably, defects introduced by Czochralski growth of doped NaCl crystals prevent execution of diffusion and therefore of the nucleation of nanocrystals. The relation of the elastic fluid effect to structural instability is also demonstrated by sample SE1 (Fig. 4). Because the sample was thermodynamically stable in the beginning of the measurements, c_{fl} was absent below T_c and appeared only at higher temperatures.

The existence of a characteristic temperature near 330 K has also been observed previously in crystal growth experiments.[8] Dissolving all nanocrystals by heating and then observing nucleation and growth at $T_{\mathrm{gr}}\geqslant 350$ K, a time dependence was observed which was governed by diffusion. The time dependence of growth changed significantly at $T_{\mathrm{gr}}=300$ K.

We believe that the fluctuations of c_{fl} shown in Fig. 4 and even stronger in Fig. 5 reflect more than just temperature effects. They may also depend on time. In this case, their observability in ultrasonic experiments stems from the extreme long time constants of relaxation processes which are connected to the diffusion of cations.

B. Elastic nonlinearity

Within the elastic model, the modification of elastic constants is obtained by expanding the relation between stress and strain beyond Hooke's law. The first additional term contains the nonlinear elastic constants of third order and bilinear combinations of strain components,

$$T_i^{(\omega)} = c_{ij}S_j^{(\omega)} + c_{ijk}S_j^{(\omega)}S_k. \tag{14}$$

Here $S_i^{(\omega)}$ denotes the strain induced at the circular frequency ω by the ultrasound. Stresses and strains without the superscript ω are referred to as spontaneous quantities. In the present subsection, we assume that the changes Δc^* above T_c are related to elastic nonlinearity. In cubic crystals, the modification of second-order stiffnesses is given by

$$c_{11}^{\mathrm{eff}} = c_{11} + (c_{111} + 2c_{112})S_0,$$

$$c_{12}^{\mathrm{eff}} = c_{12} + (2c_{112} + c_{123})S_0,$$

$$\text{or } \Delta c^* = (c_{111} - c_{123})S_0 = c^{\mathrm{nl}}S_0. \tag{15}$$

The value of the nonlinear term is given by $c^{\mathrm{nl}}=-915$ GPa.[19]

Based on Eq. (15), we consider now the changes of $c_{11}-c_{12}$ above T_c obtained for sample SE3 at 373 K. In this sample, the changes are related to the nucleation and growth of nanocrystals. Combining Eq. (11) with Eq. (15), we obtain for the concentration of $x_{\mathrm{cr}}=5\times10^{-5}$ (see Sec. IV B) a spontaneous strain of $S_0^{\mathrm{exp}}=-2.7\times10^{-4}$. This value has to be compared with theoretical estimates. As shown by Eq. (7), the decreases of ionic copper concentration will produce a positive S_0, which contradicts the experimental result. Furthermore, the maximal strain which can be produced by the decrease of x_i in sample SE3 is one order of magnitude smaller than $|S_0^{\mathrm{exp}}|$. Thus, only the mechanism outlined in Sec. II A can be relevant. Calculating the average value of S_0 for one elastic domain, we obtain for the increment Δc^*

$$\Delta c^* = c^{\mathrm{nl}}S_0^{\mathrm{model}}$$
$$= c^{\mathrm{nl}}[(a^{\mathrm{NC}}-a^M)x_{\mathrm{cr}}+a^M] = c^{\mathrm{nl}}N\left[1-\frac{C_{01}^{\mathrm{NC}}}{C_{01}^{M}}\left(\frac{R_b}{R_\alpha}\right)^3\right]x_{\mathrm{cr}}, \tag{16}$$

where N denotes the abbreviation

$$N = \frac{2(c_{11}-c_{12})^M}{C_{01}^{\mathrm{NC}} + 2(c_{11}-c_{12})^M}\frac{\Delta R}{R_0}. \tag{17}$$

Using $R_b/R_\alpha = 1$, which corresponds to a minimum of elastic deformation energy, we obtain $S_0^{\mathrm{model}} = -2.7\times 10^{-6}$. The sign is equal to the observed one but the absolute value is two orders of magnitude smaller than $|S_0^{\mathrm{exp}}|$. Now we omit the requirement of a minimal deformation energy and use S_0^{exp} to determine R_b/R_α. The result is $R_b/R_\alpha = 6.1$.

C. Interfacial stress

In the case of sample SE1, exciton spectroscopy has demonstrated that the observed decrease of Δc^* above T_c is not connected to changes of the concentration of nanocrystals. Instead, the interfacial stress decreases. Combining Eqs. (8)–(10) with Eq. (6), we obtain the following expression for the interfacial stress:

$$T_{r,0} = C_{01}^{\mathrm{NC}} N\left[1 - \frac{C_{01}^{\mathrm{NC}}}{C_{01}^{M}}\frac{3c_{11}^{M}}{C_{01}^{\mathrm{NC}} + 2(c_{11}-c_{12})^M}\left(\frac{R_b}{R_\alpha}\right)^3 x_{\mathrm{cr}}\right]. \tag{18}$$

It is reasonable to assume that for $\partial T_{r,0}/\partial T$ the same mechanism is responsible as for $\partial \Delta c^*/\partial T$. Thus Eq. (18) has to be compared with Eq. (16). Notice that for constant N, the calculated value of Δc^* is positive because c^{nl} is negative, and also the value in the large square brackets of Eq. (16) is negative because of $C_{01}^{\mathrm{NC}}/C_{01}^{M} > 1$ and $R_b/R_\alpha > 1$. As the experimental values for $\partial T_{r,0}/\partial T$ and $\partial \Delta c^*/\partial T$ are both negative, only $\partial N/\partial T$ is able to describe the common underlying mechanism. By use of the experimental results given in Eqs. (11) and (13), we obtain $\partial N/\partial T = -7.7\times 10^{-5}\ \mathrm{K}^{-1}$ and $R_b/R_\alpha = 5.8$. The latter quantity is $R_b/R_\alpha = 6.1$ in sample SE3, as shown above. The nearly perfect agreement of the values for R_b/R_α observed in both samples shows the internal consistency of the equations used. This conclusion also includes the result that the elastic continuum theory works only approximately because the relation $R_b = R_\alpha$, which fulfills the requirement of minimal elastic deformation energy, cannot be used. In spite of the large difference $S_0^{\mathrm{exp}} - S_0^{\mathrm{model}}$, the calculated displacement $u_{r,0}^{M}$ which closes the interfacial gap together with $u_{r,0}^{\mathrm{NC}}$ increases by only 6% in the case of $R_b/R_\alpha = 6$ instead of $R_b = R_\alpha$. Due to the relative smallness of the nonelastic contribution, it is understandable that the elastic continuum model remains a well-working approximation.

D. Final remarks

When we started the present work, we had knowledge about an unexplained anomalous nucleation of nanocrystals below 350 K.[8] It was not difficult to guess that in this case physical properties should show an anomaly of their dependence on temperature if measurements are performed with sufficient accuracy. This happened indeed at $T_c \approx 333$ K, and the appearance of this characteristic temperature in elastic and optical measurements indicated the common origin of changes observed at T_c. The appearance of the effect of an elastic fluid was unexpected and complicated the analysis of experimental data. It was necessary to carry out measurements on two samples existing in a quasiopposite thermodynamic state. Their different behavior below and above T_c served as a check of internal consistency of experimental results and of their interpretation.

In contrast to c_{fl}, the second additional elastic effect Δc^* shows a clear dependence on temperature. We conclude that Δc^* is produced by structural changes which are a result of the relaxation processes involved in c_{fl}. According to our results, Δc^* indicates very sensitively deviations from an elastic continuum model. Only two simple mechanisms that are absent in a homogeneously strained NaCl crystal can be responsible for the observed deviation. These are spontaneous polarization P_s and special structural changes. A new type of internal-strain parameter is able to produce both effects. Such parameters are a measure of displacements $\xi_i^{(\lambda)}$ of the atom "λ" which change its fractional coordinates,

$$\xi_i^{(\lambda)} = A_{ijk}^{(\lambda)} S_{jk} + B_{ijkl}^{(\lambda)}\frac{\partial S_{jk}}{\partial x_l}. \tag{19}$$

Notice that here the full tensor notation is used. Components $A_{ijk}^{(\lambda)}$ and $B_{ijkl}^{(\lambda)}$ are given by the site symmetry of the position occupied by atom λ and by the symmetry of the acting perturbation. Because $A_{ijk}^{(\lambda)}$ represent a tensor of third rank, they are absent for atoms that occupy a center of symmetry.[28] This is the case for all atoms in NaCl. Even nowadays, an experimental determination of the internal strain tensor $A_{ijk}^{(\lambda)}$ is difficult to achieve.[29] Therefore, it is not astonishing that the internal strain induced by a strain gradient has never been considered in the past. In contrast to the third-rank tensor A_{ijk}, the existence of the fourth-rank tensor B_{ijkl} is allowed in all crystals. For CuCl:NaCl, the second term in Eq. (19) is not only allowed by symmetry, but it also offers a reasonable explanation for the appearance of Δc^* because the strain gradient in the vicinity of a nanocrystal is huge.

For situations in which the strain gradient is parallel to the crystallographic [100] or [111] axes, it is easy to realize that $\vec{\xi}$ is a relative shift of the cation sublattice versus the anion sublattice along the gradient. The results are zigzag bonds perpendicular to and electric dipoles along the displacement. The strongest shifts occur at the interface. The modified bonding modifies elastic constants and the electric dipoles are expected to interact at the interfacial gap with the piezoelectric nanocrystal. This scenario agrees nicely with the result that changes of the parameter N are responsible for the observed effects because N depends on elastic constants and on the reduction of the interfacial gap.

A spontaneous polarization may couple via electrostriction to strain. However, the sign of the relevant coefficients of NaCl (Ref. 30) suggests elastic softening instead of the observed hardening by embedded nanocrystals. Thus, a direct impact of P_s on elastic properties is absent. The concluded mechanism which is described by $\partial N/\partial T$ [see Eqs. (16)–(18)] indicates in sample SE1 a reopening of the interfacial gap and/or a decrease of the elastic constants $c_{11}-c_{12}$. The relative magnitudes of both influences cannot be figured out reliably on the basis of the present experimental results and by using a continuum model.

VI. CONCLUSION

A comparison between experimental results and an elastic model of interactions between nanocrystal and matrix has demonstrated that the elastic continuum theory works effectively if it is slightly modified. Experimental results show that the radial stress in the vicinity of a nanocrystal decreases more strongly than predicted by the assumption of pure elastic interactions. The need for modifications arises from structural changes which are a general feature of heterogeneous materials containing embedded nanocrystals. It is proposed to describe the structural changes by internal-strain parameters which are induced by gradients of strain. One consequence of atomic displacements is the appearance of electric dipoles. Because electromechanical interactions are strong in piezoelectric materials, one may expect significant deviations from elastic continuum theory in solid solutions of III-V and II-VI semiconductors containing self-assembled quantum dots.

ACKNOWLEDGMENTS

One of us (C.P.V.) gratefully acknowledges financial support by the Deutsche Forschungsgemeinschaft.

[1] L. Banyai and S. W. Koch, *Semiconductor Quantum Dots* (World Scientific, Singapore, 1993).
[2] U. Woggon, *Optical Properties of Semiconductor Quantum Dots* Vol. 136of Springer Tracts in Modern Physics (Springer, Berlin, 1997).
[3] N. Sakakura and Y. Masumoto, Phys. Rev. B **56**, 4051 (1997); J. Zhao and Y. Masumoto, *ibid.* **60**, 4481 (1999); T. Uozumi, Y. Kayanuma, K. Yamanaka, K. Edamatsu, and T. Itoh, *ibid.* **59**, 9826 (1999); M. Ikezawa and Y. Masumoto, *ibid.* **61**, 12 662 (2000); J. Zhao, S. V. Nair, and Y. Masumoto, *ibid.* **63**, 033307 (2000); T. Itoh, K. Yamanaka, K. Edamatsu, T. Uozumi, and Y. Kayanuma, Int. J. Mod. Phys. B **15**, 3569 (2001); T. Kawazoe, K. Kobayashi, J. Lim, Y. Narita, and M. Ohtsu, Phys. Rev. Lett. **88**, 067404 (2000).
[4] C. Teichert, Phys. Rep. **365**, 335 (2002).
[5] V. A. Shchukin and D. Bimberg, Rev. Mod. Phys. **71**, 1125 (1999).
[6] V. A. Shchukin, D. Bimberg, T. P. Munt, and D. E. Jesson, Phys. Rev. Lett. **90**, 076102 (2003).
[7] U. Scholle, H. Stolz, and W. von der Osten, Solid State Commun. **86**, 657 (1993).
[8] M. Haselhoff and H.-J. Weber, Phys. Rev. B **58**, 5052 (1998).
[9] A. Migliori, J. L. Sarrao, W. M. Visscher, T. M. Bell, Ming Lei, Z. Fisk, and R. G. Leisure, Physica B **183**, 1 (1993).
[10] R. G. Leisure and F. A. Willis, J. Phys.: Condens. Matter **9**, 6001 (1997).
[11] H.-J. Weber, K. Lüghausen, M. Haselhoff, and H. Siegert, Phys. Status Solidi B **191**, 105 (1995).
[12] D. Fröhlich, M. Haselhoff, K. Reimann, and T. Itoh, Solid State Commun. **94**, 189 (1995).
[13] L. D. Landau and E. M. Lifschitz, *Theory of Elasticity* (Pergamon, New York, 1970).
[14] R. D. Shannon, Acta Crystallogr., Sect. A: Cryst. Phys., Diffr., Theor. Gen. Crystallogr. **32**, 751 (1976); J. Ziolkowski, J. Solid State Chem. **57**, 269 (1985).
[15] J. Schreuer, IEEE Trans. Ultrason. Ferroelectr. Freq. Control **49**, 1474 (2002).
[16] K. Reimann and St. Rübenacke, Phys. Rev. B **49**, 11 021 (1994).
[17] M. Haselhoff, K. Reimman, and H.-J. Weber, Eur. Phys. J. B **12**, 147 (1999).
[18] M. Haselhoff and H.-J. Weber, Mater. Res. Bull. **30**, 607 (1995).
[19] A. G. Every and A. K. McCurey, *Second and Higher Order Elastic Constants*, edited by D. F. Nelson, Landolt-Börnstein, New Series III/29a (Springer, Berlin, 1992).
[20] S. Yamamoto, I. Ohno, and O. L. Anderson, J. Phys. Chem. Solids **48**, 143 (1987).
[21] K. Fussgänger, Phys. Status Solidi **34**, 157 (1969).
[22] Al. L. Efros and A. L. Efros, Sov. Phys. Semicond. **16**, 772 (1982).
[23] A. E. Ekimov, A. A. Onushchenko, A. G. Plykhin, and Al. L. Efros, Sov. Phys. JETP **61**, 891 (1985).
[24] T. Itoh, Y. Iwabuchi, and M. Kataoka, Phys. Status Solidi B **145**, 567 (1988).
[25] P. M. Valov, L. V. Gracheva, L. V. Leiman, and T. A. Negovorova, Phys. Solid State **36**, 954 (1994).
[26] M. V. Kurik, Phys. Status Solidi A **8**, 9 (1971).
[27] W. J. Dunning and E. Hornbogen, in *Nucleation*, edited by A. C. Zettlemoyer (Marcel Dekker, New York, 1969).
[28] M. Born and K. Huang, *The Dynamical Theory of Crystal Lattices* (Oxford University Press, Oxford, 1966).
[29] H.-J. Weber, Phys. Rev. B **51**, 12 209 (1995).
[30] J. Schreuer and S. Haussühl, J. Phys. D **32**, 1263 (1999).